Molecular BioSystems

Cite this: *Mol. BioSyst.*, 2011, **7**, 3223–3233

www.rsc.org/molecularbiosystems

PAPER

Characterization of ubiquitination dependent dynamics in growth factor receptor signaling by quantitative proteomics†

Vyacheslav Akimov, Kristoffer T. G. Rigbolt, Mogens M. Nielsen and Blagoy Blagoev*

Received 8th July 2011, Accepted 30th August 2011
DOI: 10.1039/c1mb05185g

Protein ubiquitination is a dynamic reversible post-translational modification that plays a key role in the regulation of numerous cellular processes including signal transduction, endocytosis, cell cycle control, DNA repair and gene transcription. The conjugation of the small protein ubiquitin or chains of ubiquitin molecules of various types and lengths to targeted proteins is known to alter proteins' lifespan, localization and function and to modulate protein interactions. Despite its central importance in various aspects of cellular life and function there are only a limited number of reports investigating ubiquitination on a proteomic scale, mainly due to the inherited complexity and heterogeneity of ubiquitination. We describe here a quantitative proteomics strategy based on the specificity of ubiquitin binding domains (UBDs) and Stable Isotope Labeling by Amino acids in Cell culture (SILAC) for selectively decoding ubiquitination-driven processes involved in the regulation of cellular signaling networks. We applied this approach to characterize the temporal dynamics of ubiquitination events accompanying epidermal growth factor receptor (EGFR) signal transduction. We used recombinant UBDs derived from endocytic adaptor proteins for specific enrichment of ubiquitinated complexes from the EGFR network and subsequent quantitative analyses by high accuracy mass spectrometry. We show that the strategy is suitable for profiling the dynamics of ubiquitination occurring on individual proteins as well as ubiquitination-dependent events in signaling pathways. In addition to a detailed seven time-point profile of EGFR ubiquitination over 30 minutes of ligand stimulation, our data determined prominent involvement of Lysine-63 ubiquitin branching in EGF signaling. Furthermore, we found two centrosomal proteins, PCM1 and Azi1, to form a multi-protein complex with the ubiquitin E3 ligases MIB1 and WWP2 downstream of the EGFR, thereby revealing possible ubiquitination cross-talk between EGF signaling and centrosomal-dependent rearrangements of the microtubules. This is a general strategy that can be utilized to study the dynamics of other cellular systems and post-translational modifications.

Introduction

Protein ubiquitination is a widespread reversible post-translational modification that is used by eukaryotic cells as a major regulatory mechanism to alter protein stability, localization, conformation and activity of the modified substrates. Conjugation of ubiquitin to target proteins requires a series of enzymatic reactions involving activating (E1) and conjugating (E2) enzymes as well as ubiquitin ligases (E3) which determines the specificity of ubiquitin attachment.[1] Ubiquitin itself can also undergo ubiquitination on any of its seven lysine residues resulting in the formation of distinct poly-ubiquitin chains.[2] Depending on the number and type of ubiquitin moieties attached, a protein can be mono-ubiquitinated, multiple mono-ubiquitinated at different lysines and poly-ubiquitinated. This heterogeneity plays a critical role in molecular recognition of the modified proteins by numerous types of ubiquitin binding proteins.[3] In addition, the size and type of ubiquitin conjugates serve as specific codes for determination of the fate of tagged proteins. For example, modification by Lysine-48 poly-ubiquitin chains directs proteins mainly for degradation by the 26S proteasome, whereas mono-ubiquitination and Lysine-63 type poly-ubiquitination have been associated with regulation of several cellular processes including signal transduction, endocytosis, chromatin rearrangement and DNA repair.[4–7] Ubiquitination is also a central component of the

Center for Experimental BioInformatics (CEBI), Department of Biochemistry and Molecular Biology, University of Southern Denmark, Campusvej 55, DK-5230 Odense M, Denmark. E-mail: bab@bmb.sdu.dk; Fax: +45 6593 3018; Tel: +45 6550 2366
† Electronic supplementary information (ESI) available: Six figures and six tables. See DOI: 10.1039/c1mb05185g

signaling pathways controlled by growth factors and their cognate receptors, the receptor tyrosine kinases (RTKs). Growth factor signaling modulates a wide range of cellular processes such as survival, proliferation, differentiation and motility.[8–10] RTK signal transduction involves cascades of phosphorylation events where the intensity and duration of the signal are to a large extent controlled by endocytosis of the activated receptor complex and its ultimate degradation in the lysosomes.[11–13] The ubiquitination of RTKs is pivotal to this highly dynamic chain of events, serving as a signal for its internalization into early endosomes and for further endocytic sorting. Various endocytic adaptor proteins such as Eps15, Epsin, Hrs and STAM also play important roles in this process. These adaptors bind specifically to the ubiquitinated receptor *via* their ubiquitin-binding domains (UBDs) and guide the subsequent trafficking of ubiquitinated cargo through the endocytic compartments.[11,14,15] Moreover, the ubiquitin-binding proteins themselves undergo reversible mono-ubiquitination, which in turn regulate their functions.[16]

Because of the complex nature of ubiquitination, its heterogeneity and the lack of suitable procedures there is a need for new strategies to study ubiquitination on a proteomic scale and strategies for targeting selectively a subset of ubiquitination events involved in specific processes.[17] As a consequence of these challenges there are still a limited number of reports investigating protein ubiquitination on a proteomic scale. Mass spectrometric approaches have mainly been limited to affinity enrichment of ubiquitinated proteins using over-expressed tagged ubiquitin[18–21] or poorly-working antibodies raised against ubiquitin.[21–23] Recently, Xu *et al.* described a more elegant strategy to enrich directly modified peptides from ubiquitinated targets using antibodies against the remnant diglycine of ubiquitin on lysine residues after tryptic digestion.[24] Due to the low expression levels of signaling proteins and low stoichiometry of ubiquitination on these proteins, it is even more challenging to separate the ubiquitinated proteins and ubiquitination-dependent processes involved in a specific cellular pathway from all ubiquitination events that take place in the cell. Some encouraging results in this respect have been presented in earlier proteomic studies utilizing immobilized UBDs from the ubiquitin-binding protein p62.[25,26]

Here we provide a strategy for monitoring the dynamics of ubiquitination events involved in signaling networks. We have applied this approach to characterize the temporal dynamics of ubiquitination-dependent events in EGFR signaling. The strategy utilizes selective enrichment of ubiquitinated complexes from the EGFR pathway using recombinant UBDs as a bait and quantitative proteomics based on Stable Isotope Labeling by Amino acids in Cell culture (SILAC).[27]

Results

Identification and quantitation of ubiquitination dynamics in the EGFR signaling network

To characterize ubiquitination-dependent events in the EGFR signaling network and profile their dynamic regulation over time we applied a combination of affinity purification using GST-tagged UBDs and SILAC-based quantitative mass spectrometry (Fig. 1A). Three populations of HeLa cells were "double–triple" labeled with three isotopically distinct versions of Lysine and Arginine,[28,29] stimulated with the EGF for three time-points and mixed. Prior to the enrichment step, abundant Lys-48 poly-ubiquitin protein conjugates were depleted from the lysates using GST-UBA domains of human Rad23A (hHR23A).[30] We verified that this pre-cleaning step did not alter the level of the EGFR in the cellular lysates (ESI†, Fig. S1). To enrich ubiquitinated protein complexes the pre-cleaned lysates were incubated with recombinant GST-tagged UBDs from the endocytic adaptor proteins Eps15 and Epsin-1. Samples enriched in ubiquitinated proteins and their bound interaction partners were separated by 1D gel electrophoresis, digested with trypsin and analyzed by nanoscale liquid chromatography coupled to tandem mass spectrometry (LC-MS/MS) on a high-resolution and mass accuracy instrument (LTQ-FT Ultra, Thermo Scientific). By repeating the experiment for another two triplets of time-points and using a common time point for all three sets of experiment, we generated a detailed seven time-point dynamic profile of ubiquitination-dependent events in the EGFR signaling network (Fig. 1B).

We applied stringent criteria for protein identifications including at least two unique peptides and a Mascot protein score higher than 70. Using these criteria we identified 324 proteins co-precipitating with the recombinant ubiquitin-binding domains (ESI†, Table S1), with an average mass accuracy of the entire dataset below 1 ppm (ESI†, Table S2). There were no matches to the reverse database fulfilling our protein identification criteria indicating that our false discovery rate was below 1%. Regarding SILAC quantitation, the average relative standard deviation for the entire dataset was 11.1%. Based on this calculation, we classified a regulated protein if it had a SILAC ratio above 1.5 fold in at least one time point, corresponding to a difference of more than four average standard deviations. From the list of proteins for which a complete time-course profile could be obtained, twelve proteins were regulated beyond the 1.5 fold regulation cut-off (summarized in Table 1).

An independent biological experiment was performed using the above described experimental workflow (ESI†, Tables S3 and S4). In these experiments, however, cells were serum-deprived for a longer time prior to EGF stimulation (see Experimental procedures) resulting in lower basal levels of protein ubiquitination in the non-stimulated cells. Consequently we observed higher SILAC ratios for the regulated proteins upon EGF stimulation, reflecting the larger fold change compared to the non-stimulated control cells. Nevertheless, there was an overall very good correlation of the measured protein ratios between the two experiments with an average Pearson correlation coefficient of 0.93 (ESI†, Fig. S2). Importantly, the dynamic profiles of ubiquitinated proteins between the two experiments were very similar, despite the expected differences in the maximum fold change of regulation (ESI†, Fig. S3).

EGFR ubiquitination dynamics

The occurrence of multiple ubiquitinations on the EGFR and the importance of this modification for the downstream signal

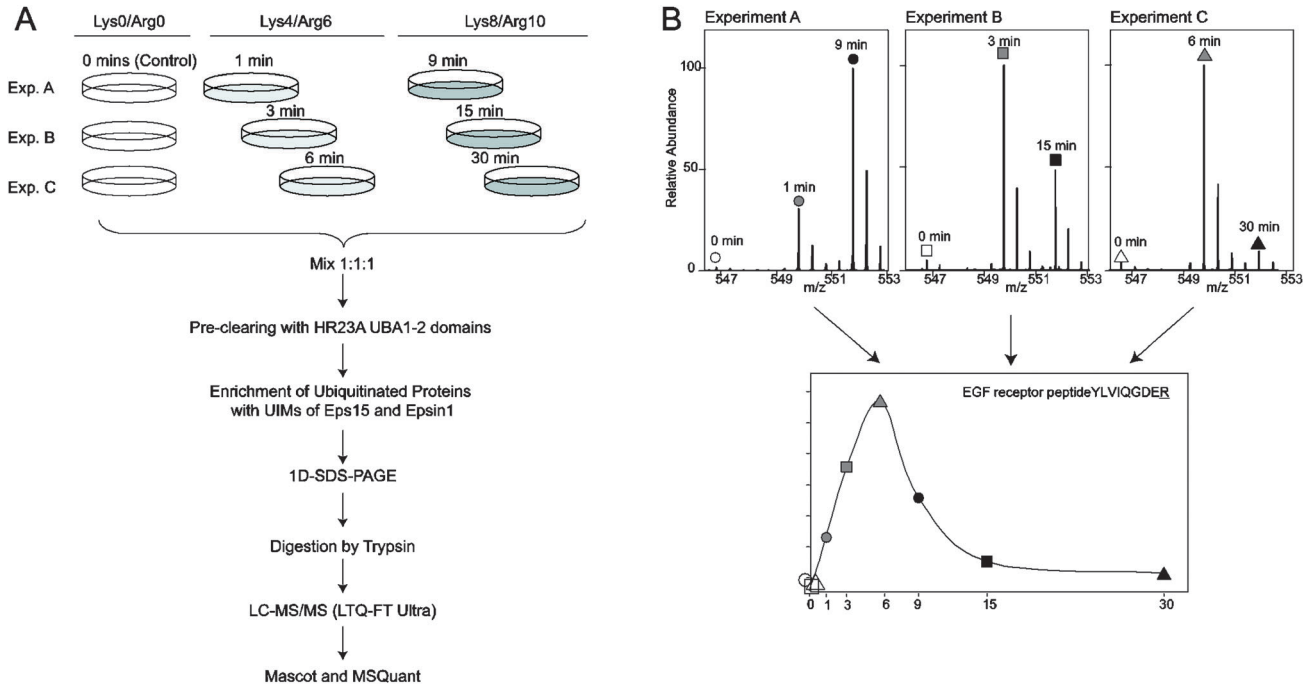

Fig. 1 Strategy for characterization of ubiquitination dependent dynamics in EGFR signaling by quantitative proteomics. (A) To identify ubiquitinated proteins cells were "double–triple" SILAC labeled with Lysine and Arginine and stimulated with EGF for the specified times. Ubiquitinated protein complexes from the premixed cellular lysates were enriched by a two-step procedure using recombinant GST-tagged UBDs as indicated, separated by 1D gel electrophoresis, digested with trypsin and analyzed by LC-MS/MS. (B) Repeating the complete experiment for three sets of time-points with a common reference time-point allowed the creation of detailed seven step time-course profiles. The example is given with the doubly charged peptide YLVIQGDER derived from the EGFR.

Table 1 List of regulated proteins displaying ubiquitination mediated dynamics upon EGF stimulation

		Protein ratio					
Acc. key	Gene name	1 min	3 min	6 min	9 min	15 min	30 min
IPI00018274.1	EGFR	17.9 ± 1.4	25.3 ± 2.1	37.9 ± 3.2	15.8 ± 1.7	12.8 ± 1.5	3.22 ± 0.98
IPI00292856.4	CBLB	4.79 ± 0.60	4.88 ± 0.47	4.38 ± 0.82	3.14 ± 0.51	2.67 ± 0.34	0.89 ± 0.07
IPI00154910.4	STS-1	2.24 ± 0.16	3.42 ± 0.06	3.03 ± 0.13	1.69 ± 0.03	2.27 ± 0.26	1.41 ± 0.22
IPI00006213.2	PCM1	0.91 ± 0.08	0.79 ± 0.08	0.96 ± 0.08	2.12 ± 0.22	2.51 ± 0.29	1.51 ± 0.14
IPI00784402.1	AZI1	0.98 ± 0.07	0.72 ± 0.12	0.98 ± 0.10	2.19 ± 0.24	2.30 ± 0.11	1.36 ± 0.09
IPI00256684.1	AP2A1	1.47 ± 0.20	1.67 ± 0.20	1.71 ± 0.20	1.78 ± 0.10	1.74 ± 0.23	1.21 ± 0.15
IPI00784156.1	AP2B1	1.18 ± 0.07	1.39 ± 0.03	1.12 ± 0.11	1.55 ± 0.14	1.55 ± 0.05	1.11 ± 0.13
IPI00020127.1	RPA1	1.00 ± 0.09	1.34 ± 0.10	1.72 ± 0.27	1.58 ± 0.06	1.50 ± 0.27	1.52 ± 0.06
IPI00163321.5	NEDD4L	1.06 ± 0.09	1.12 ± 0.20	1.30 ± 0.26	1.36 ± 0.13	1.70 ± 0.11	1.18 ± 0.06
IPI00183054.1	MIB1	0.91 ± 0.08	0.91 ± 0.10	0.90 ± 0.17	1.24 ± 0.09	1.52 ± 0.20	1.09 ± 0.16
IPI00013010.6	WWP2	0.87 ± 0.16	1.19 ± 0.05	0.99 ± 0.20	1.03 ± 0.15	1.53 ± 0.07	1.09 ± 0.03
IPI00008477.1	TPX2	1.29 ± 0.16	1.51 ± 0.34	1.46 ± 0.14	1.25 ± 0.34	1.37 ± 0.22	1.35 ± 0.19

transduction are well appreciated.[15,31] Indeed, the highest ubiquitination response in our dataset was found for EGFR (Table 1) with a strong peak close to 40 fold above the basal level after 6 minutes, followed by a slow decay (Fig. 2A). We compared the profile from our mass spectrometry based strategy with immunoblotting and found a close correlation between the profiles obtained with these complementary approaches (Fig. 2B). In addition to the profiles for the overall ubiquitination dynamics of EGFR we also identified two ubiquitination sites on Lys-716 and Lys-737 (ESI†, Fig. S4) that are known to be some of the major sites of EGFR ubiquitination.[32]

From the gel segment containing EGFR we also identified several peptides from ubiquitin itself including four diglycine peptides derived from ubiquitin branching *via* lysines 6, 11, 48 and 63 (ESI†, Fig. S5). The ubiquitin peptides corresponding to Lys-6, Lys-11 and Lys-48 chains showed only insignificant fluctuations over the time-course of stimulation whereas the peptide reflecting Lys-63 branching displayed a profile with a pattern similar to the one observed for the EGFR (Fig. 2C). Previous studies have already suggested direct involvement of Lys-63 branching in the ubiquitination of EGFR,[32] which was the most plausible explanation for our observation as well. It was however possible that the increase in Lys-63 chains might arise due to such modified proteins co-migrating in the same gel band as the EGFR. We therefore performed additional experiments using antibodies specifically recognizing Lys-63 poly-ubiquitin chains, which also resulted in detectable Lys-63

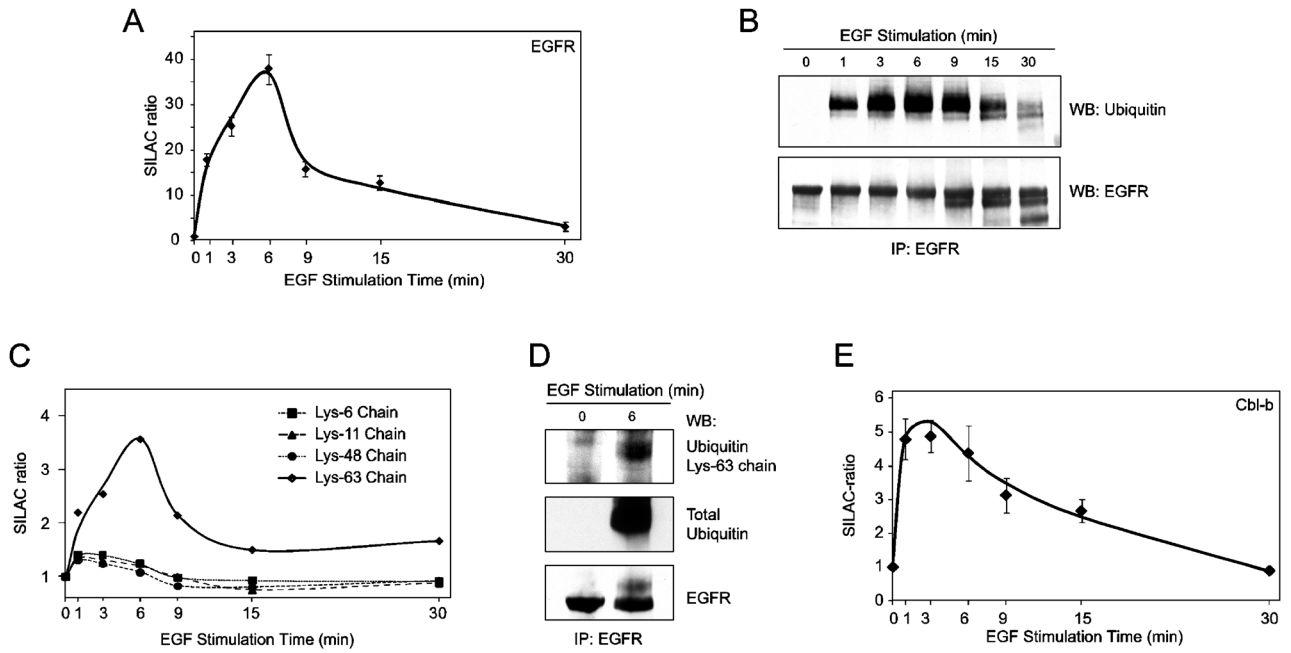

Fig. 2 Ubiquitination dynamics associated with EGFR. (A) Profile of the ubiquitination mediated regulation of EGFR determined by quantitative proteomics. (B) EGFR ubiquitination profile by immunoprecipitation and Western blotting. (C) Regulation of branched poly-ubiquitin chains identified from the same gel band as EGFR. (D) Assessment of Lys-63 polyubiquitination on EGFR. Western blotting was performed using antibodies specific to Lys-63-linkage polyubiquitin (top panel) as well as total ubiquitin for comparison (middle panel). (E) Profile of the ubiquitination dependent dynamics of Cbl-b in response to EGF stimulation as determined by quantitative proteomics.

ubiquitin branching on the receptor in response to EGF treatment (Fig. 2D). Nevertheless, the dramatic difference in the magnitude of total EGFR ubiquitination (Fig. 2A) and branched ubiquitin peptides (Fig. 2C) clearly indicates that EGFR ubiquitination is predominantly composed of multiple mono-ubiquitinations[33,34] and only a small fraction can be assigned to Lys-63 chains. It should be noted however that a possible involvement of Lys-48 branching cannot be entirely excluded since a large fraction of Lys-48 ubiquitinated proteins were depleted from the cellular lysates by the UBA domains of hHR23A, although the amount of ubiquitinated EGFR appeared to be unaffected from this pre-clearing step (ESI†, Fig. S1).

Dynamics of ubiquitin ligases

The ultimate event in protein ubiquitination is the covalent attachment of ubiquitin to the target proteins, a process performed by the family of E3 ligases, which also confer substrate specificity. Similar to endocytic adaptor proteins, many E3 ligases are also commonly modified with ubiquitin and this reversible mono-ubiquitination strictly controls their actions.[14,35] We identified EGF-dependent regulation of four distinct members of the E3 ligase family, namely Cbl-b, Nedd4L (also known as Nedd4-2), Mib1 and WWP2 (Table 1). The involvement of Cbl and Nedd4 ligases in EGFR signaling is well studied,[14,15] whereas Mib1 and WWP2 have not previously been implicated in EGFR signal transduction. Cbl is recruited to the activated EGFR by means of its phosphotyrosine interaction domain and subsequently ubiquitinates the receptor. Correspondingly, we find a rapid increase in Cbl-b reflecting well the current understanding that Cbl is the main E3 ligase responsible for the ubiquitination of the EGFR upon receptor activation (Fig. 2E).[15,36] In contrast, Nedd4 and Nedd4L ligases target signaling proteins downstream of the receptor such as ACK1, Eps15 and Cbl,[35,37,38] which is supported by a delayed onset in the Nedd4L time-course profile with a peak after 15 minutes (Table 1). We are not aware of previous reports implicating Mib1 and WWP2 in EGFR signaling and were thus intrigued to find regulated profiles for these E3 ligases. Both proteins show a time-course profile highly similar to the one observed for Nedd4L peaking at 15 minutes (Table 1) and it could thus also be expected that they target proteins downstream of the EGFR.

Ubiquitin dependent cross-talk between growth factor signaling and centrosome assembly

Applying mass spectrometry based strategies to study ubiquitination also provides the potential for unbiased identification of novel ubiquitination targets. A case in point is our identification of the proteins Pericentriolar material 1 (PCM1) and 5-azacytidine-induced protein 1 (Azi1; also known as Cep131), which were similarly regulated by the EGF with a delayed onset of ubiquitination with a maximum after 15 minutes (Fig. 3A). These proteins are known to play a role in centrosome assembly and function[39,40] but have not previously been reported to be involved in receptor tyrosine kinase signaling, and only recently been shown to be ubiquitinated.[20] Because of the established involvement of PCM1 in microtubule organization we first examined the possibility of direct interaction of PCM1 with activated EGFR complexes during endocytic transport, which could account for the observed PCM1 regulatory profile. However, immunofluorescent

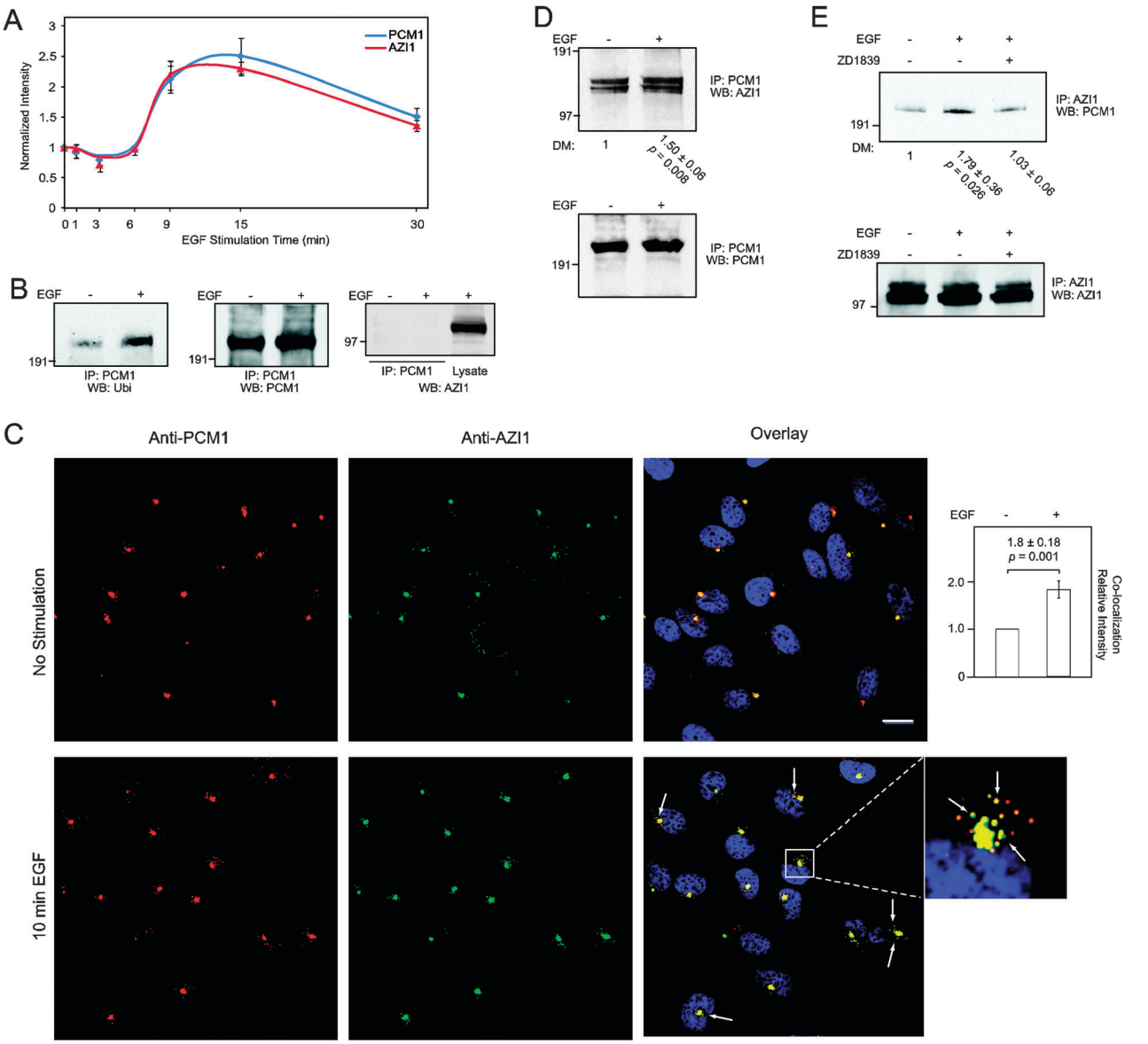

Fig. 3 Centrosomal proteins PCM1 and AZI1 are novel components of ubiquitination dependent EGFR signaling. (A) Time-course profile of the ubiquitin mediated regulation of PCM1 and Azi1 as determined from quantitative proteomics. (B) Induced ubiquitination of PCM1 in response to the EGF. Proteins in the cellular lysates were denatured using 1% SDS prior to PCM1 immunoprecipitation. Panel on the left shows the efficiency of 'striping' co-precipitating proteins due to SDS treatment. (C) Co-localization of PCM1 (red) and AZI1 (green) by immunofluorescent confocal microscopy. Cellular nuclei are visualized by DAPI staining and displayed only in the overlay images. Scale bars, 15 μm. Arrows indicate additional co-localization of PCM1 and AZI1 upon EGF stimulation in smaller perinuclear loci. Panel on the right top shows quantitation of the relative intensity of co-localization normalized to non-stimulated cells (n = 3, error bar represents Standard Deviation). (D, E) Reciprocal co-immunoprecipitation of PCM1 and AZI1. Numbers below top panels indicate the relative amounts of AZI1 (panel D, n = 4) and PCM1 (panel E, n = 3) respectively, compared to the non-stimulated as obtained by density measurements. (E) The EGF-dependent increased association of PCM1 and AZI1 requires EGFR kinase activity. ZD1839 (Iressa)—EGFR tyrosine kinase inhibitor.

microscopy did not reveal detectable co-localization of the EGFR with PCM1 following EGF stimulation (data not shown).

We therefore investigated if PCM1 itself becomes ubiquitinated upon ligand stimulation and indeed observed pronounced EGF-dependent ubiquitination of PCM1 (Fig. 3B). Since PCM1 and Azi1 displayed very similar ubiquitination-dependent profiles after EGF stimulation (Fig. 3A) we set to investigate possible binding of these two proteins. Immunofluorescent experiments using confocal microscopy revealed that PCM1 and Azi1 co-localize at granule-like structures in the perinuclear area even in the absence of EGF treatment (Fig. 3C). The intensity of co-localization however increased further by 1.8 fold in response to the EGF and intriguingly spread to additional smaller foci in the vicinity of the centrosomes. Similar results were obtained from reciprocal co-immunoprecipitation and Western blotting experiments showing constitutive binding with 1.5–1.8 fold increased association of the two proteins upon ligand stimulation (Fig. 3D and E). Repeating this experiment in the presence of the EGFR

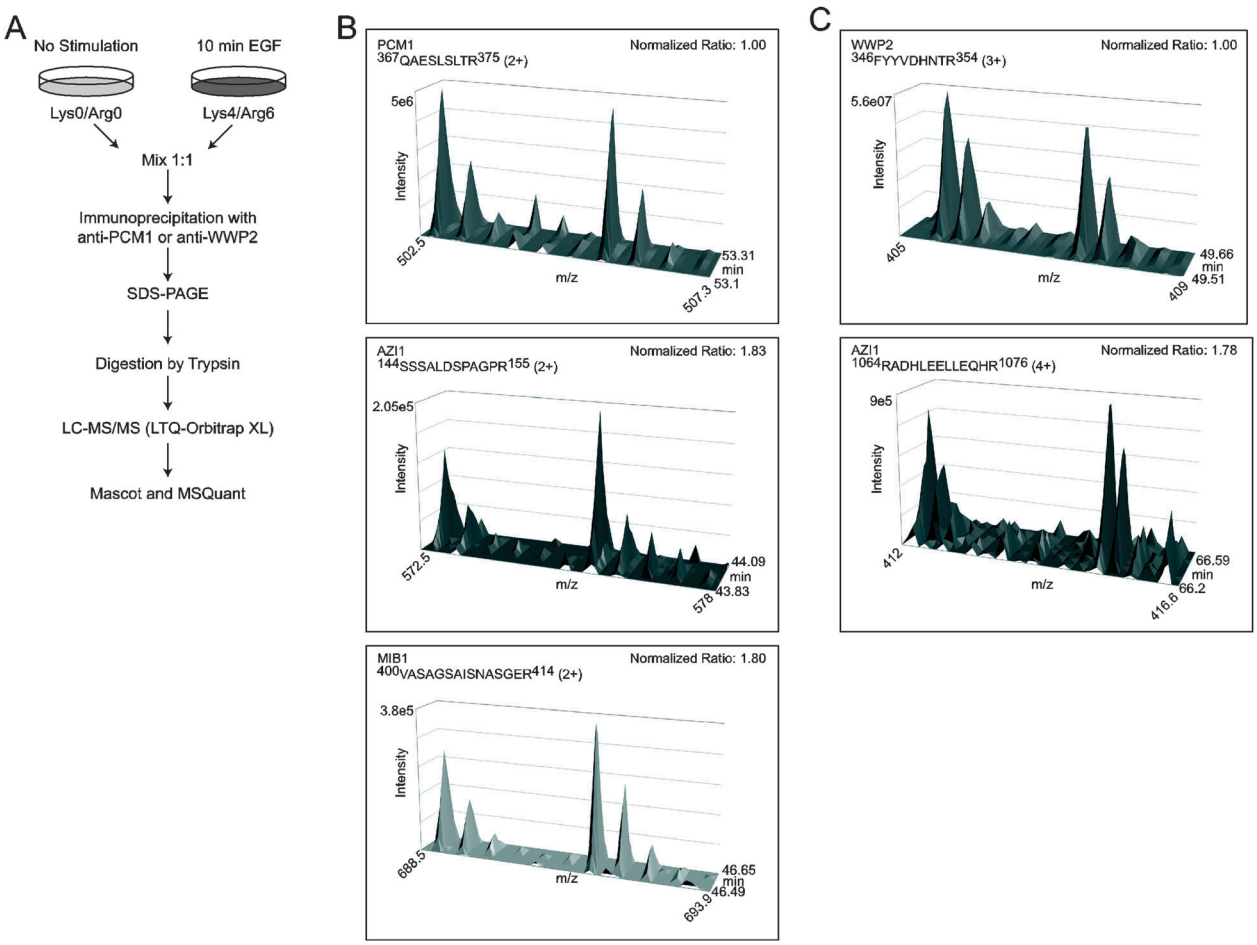

Fig. 4 Identification of PCM1 and WWP2 interaction partners by quantitative proteomics. (A) Differentially SILAC-labeled cells were either left untreated or stimulated with EGF for 10 min. PCM1 or WWP2 and their interacting proteins were enriched by immunoprecipitation with antibodies to PCM1 or WWP2, respectively. Precipitated proteins were separated by SDS-PAGE and analyzed by LC-MS/MS. Representative precursor spectra showing (B) increased association of PCM1 with AZI1 and MIB1 and (C) WWP2 increased interaction with AZI1 upon EGF stimulation.

tyrosine kinase inhibitor ZD1839 (Iressa) revealed that the observed increase in binding between PCM1 and Azi1 is specific to EGF stimulation and requires EGFR activation (Fig. 3E).

To consolidate this finding we combined affinity purification with the quantitative proteomics approach[41] to identify EGF-induced specific interaction partners for PCM1 (Fig. 4A). Briefly, two parallel cell cultures were SILAC labeled and either left untreated or stimulated with the EGF for 10 minutes. Endogenous PCM1 and interacting proteins were enriched by immunoprecipitation with the PCM1 antibody, precipitated proteins were separated by SDS-PAGE and analyzed by LC-MS/MS. This experiment resulted in the identification of several candidates including Azi1 (ESI†, Tables S5 and S6). In correlation with our previous observation, Azi1 displayed a 1.83 fold increased association with PCM1 as a result of EGF treatment of the cells (Fig. 4B). Interestingly, the E3 ligase MIB1 was also identified in this unbiased screen and displayed similar increase in binding to PCM1 upon EGF stimulation (Fig. 4B). Subsequent immunostaining experiments confirmed this finding, showing specific co-localization of PCM1 and MIB1 at the granule-like structures close to the nucleus (Fig. 5A). Considering the high similarity of the ubiquitination dependent profiles of MIB1 and WWP2 (Table 1) and the observation that MIB1 takes part in the same protein complex as PCM1 and Azi1, we performed additional experiments focused on WWP2 using again confocal microscopy as well as SILAC-based affinity purification. The results demonstrated an increased interaction of WWP2 with Azi1 upon EGF stimulation (Fig. 4C and ESI†, Table S5) and clear co-localization with PCM1 in the perinuclear area (Fig. 5B). Taken all together, the data illustrate that PCM1, Azi1 and the E3 ligases MIB1 and WWP2 all take part in one multi-protein complex.

Discussion

Large-scale studies using high accuracy quantitative proteomics have proven very beneficial for comprehensive characterization of complex signaling networks by means of phosphorylation.[42–44] Although bearing the same potential for systematic characterization of protein ubiquitination, quantitative proteomics have not been effectively exploited in this field mainly due to the lack of suitable tools and strategies. We provide here a novel approach for selective decoding of ubiquitination dependent

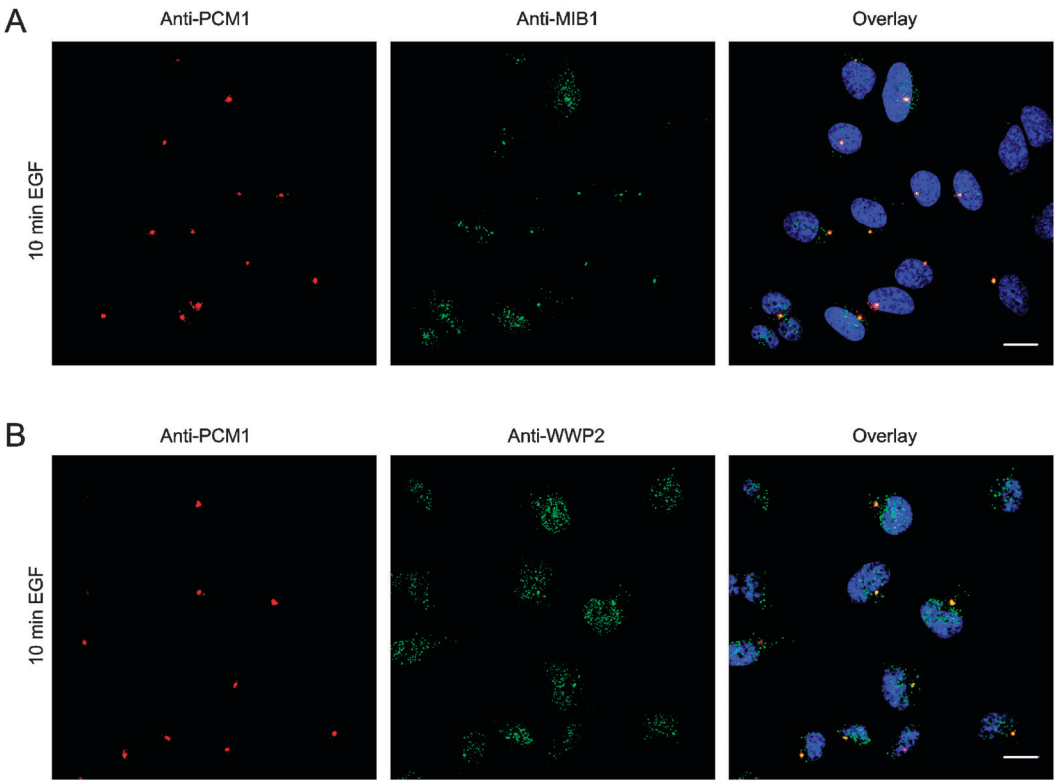

Fig. 5 Association of PCM1 with the E3 ubiquitin ligases MIB1 and WWP2. Co-localization of (A) PCM1 (red) with MIB1 (green) and (B) PCM1 (red) with WWP2 (green) by immunofluorescent confocal microscopy. Cellular nuclei are visualized by DAPI staining and displayed only in the overlay images. Scale bars, 15 μm.

processes in signaling networks taking advantage of the selectivity of UBDs and SILAC-based quantitative proteomics. We show that the strategy is suitable for profiling the dynamics of ubiquitination occurring on individual proteins as well as ubiquitination-driven events in signaling pathways. It is intriguing to point out that we have previously identified regulated phosphorylations in response to the EGF on most of the proteins that we now found with ubiquitination-dependent dynamics. These include EGFR, CblB, Sts1, PCM1, Azi1, Nedd4L and TPX2,[16,28] highlighting the crosstalk between phosphorylation and ubiquitination, and the extent of the combinatorial use of these PTMs for regulating proteins' activities and functions in the process of signal transduction.[45]

In previous studies centered on phosphotyrosine-directed signaling upon EGF stimulation, we have indirectly extrapolated the dynamics of ubiquitinated EGFR based on the changes in abundance of the ubiquitin peptides derived from the same gel band as the receptor.[46] It is noteworthy that the profile of receptor ubiquitination determined from this conceptually different approach closely correlates with our current assessment. In addition, our current study provided insights into the disputed involvement of Lys-63 chains in the ubiquitination of the EGFR. The dynamic changes of Lys-63 branched ubiquitin peptides in response to the EGF indicate clear contribution of Lys-63 conjugates in EGFR signaling, along with the more prominent mono-ubiquitination.

Another intriguing observation arose from the notable absence in our list of identified proteins of ErbB2, which is regarded as the preferred dimerization partner of the EGFR when both receptors are present in the cell.[47] In accordance with this notion, we have readily identified phosphorylated ErbB2 from EGF stimulated HeLa cells[28,46] as well as from other cell lines co-expressing both receptors.[48,49] However, we did not detect ErbB2 in the pulled-down ubiquitinated complexes despite the strong presence of EGFR in these samples. This observation would therefore indicate very low ubiquitination of the EGFR–ErbB2 heterodimers upon EGF stimulation, which is well in line with previous reports suggesting that EGFR–ErbB2 complexes are only modestly ubiquitinated and thus less prone to endocytosis and ultimately degradation.[50–52]

The use of an MS-based approach also permits the unbiased identification of new ubiquitination-dependent protein complexes and direct ubiquitin targets. We determined that the centrosomal proteins, PCM1 and Azi1, and the E3 ligases, MIB1 and WWP2, all belong to one multi-protein complex around the MTOC (microtubule organizing center). PCM1 and Azi1 are known to be important for centrosome assembly and microtubule nucleation[39,40] and both MIB1 and WWP2 have been associated with several aspects of cellular trafficking.[53–55] It is therefore tempting to speculate that this novel complex is possibly involved in the EGF-induced reorganization of the microtubules that is required for the endocytic trafficking, with ubiquitination playing an important role in this dynamic process.

In a recent study by Argenzio *et al.*,[21] the authors used SILAC-based quantitative proteomics in combination with ubiquitin antibodies to investigate ubiquitination in HeLa cells following 10 min EGF stimulation. More than 1000 potentially

ubiquitinated proteins were identified in this screen with 34 proteins displaying more than 1.5 fold increase in the SILAC ratio in response to the EGF. In general, we found a big overlap between the proteins identified in the current study and the ones presented in Argenzio *et al*. Nevertheless, despite the larger list of Agenzio *et al*., there were a considerable number of proteins solely identified by our approach (ESI†, Fig. S6). Notably, these included the ubiquitin E3 ligases MIB1 and WWP2, indicating complementary strengths of the two approaches for unbiased investigation of endogenous ubiquitination events.

Taken together, we described the utility of a combinatorial quantitative proteomics strategy for selective enrichment and characterization of ubiquitinated sub-proteomes. Although we have focused our studies on EGFR signaling, this approach is not restricted to the ubiquitination events accompanying RTK signal transduction. It is a generic strategy that can be applied to other cellular functions and systems by selecting appropriate UBDs from proteins known to be involved in the corresponding processes of interest. Furthermore, it is becoming more apparent that other PTMs, like for example lysine acetylation,[56–59] play more prominent roles in RTK signaling than anticipated so far. The dynamics and regulation of various PTMs could be investigated in an essentially identical way as described in the current study, taking advantage of the specificity of the different protein interaction domains that recognize these modifications.[11,60]

It should be noted that an important factor for designing a successful strategy similar to the one described here is the selection of suitable protein interaction domains for the enrichment step. Many UBDs do not display the same affinity and specificity towards their cognate binding partners in isolation (for example as GST-fusions) as they have in full protein context in the cell. Some UBDs are also involved in proteins' dimerization, independent of their ubiquitin binding function, and are not ideal for such enrichment approaches.[61,62] Other UBDs require cooperation from additional domains within the protein for stable binding to their physiological ubiquitinated partners and display only poor binding to ubiquitinated proteins when used in isolation.[63]

Experimental

DNA constructs

The plasmid pGEX-6P-1 (Amersham Pharmacia Biotech), containing a 165 bp fragment encoding the UIM1 and UIM2 domains in tandem of human Eps15 (amino acids 842–897), was kindly provided by Prof. Ivan Dikic (Goethe University Medical School, Frankfurt, Germany). The constructs containing the UIM1 and UIM2 domains in tandem of human Epsin1 (a.a. 183–227) as well as the UBA1 (a.a. 161–201) and UBA2 (a.a. 318–358) domains of hHR23A were made by PCR amplification and cloning into plasmid pGEX-4T1 in-frame with glutathione *S*-transferase (GST). The GST fusion proteins were expressed in *Escherichia coli* and purified on glutathione Sepharose beads as previously described.[64]

Cell culture and affinity purification

For SILAC labeling experiments three populations of HeLa (human cervix epithelial adenocarcinoma) cells were grown in DMEM medium and differentially encoded with L-arginine (Arg0) and L-lysine (Lys0), L-arginine–$^{13}C_6$ $^{14}N_4$ (Arg6) and L-lysine–$^{2}H_4$ (Lys4), or L-arginine–$^{13}C_6$ $^{15}N_4$ (Arg10) and L-lysine–$^{13}C_6$ $^{15}N_2$ (Lys8) as described previously.[28,65] Five 15 cm dishes per condition were grown to 90% confluence of the cells, serum starved for 12 h and stimulated with 150 ng ml^{-1} EGF for 0 (Lys0/Arg0 cells), 1 (Lys4/Arg6 cells) and 9 (Lys8/Arg10 cells) min. Two other sets of identically labeled cells were treated with EGF for 0, 3, 15 and 0, 6, 30 min correspondingly (see Fig. 1). Cells from all conditions were lysed in ice-cold lysis buffer containing 1% (v/v) Triton X-100, 150 mM NaCl, 20 mM Tris, pH 8.0, 1 mM EDTA, 1 mM sodium orthovanadate and protease inhibitors (Complete tablets, Roche). Lysates were centrifuged for 12 min at 14 000*g* to pellet cellular debris and the supernatant was mixed in a 1 : 1 : 1 protein ratio. To pre-clear lysates from proteins targeted for proteasomal degradation a mixture of recombinant UBA1 and UBA 2 domains of hHR23A (100 μg GST-fusion proteins) bound to glutathione-Sepharose beads was used. Lysates were precleared for 45 min and then incubated with a mixture of Sepharose immobilized GST-UIMs of hEpsin1 and hEps15 (75 μg each). After 6 h of incubation beads were washed extensively with lysis buffer, boiled in SDS sample buffer for 10 min at 90 °C and resolved on Novex 4–12% Bis-TRIS gradient gel using the MOPS buffer system (Invitrogen). To visualize proteins the gel was stained with the Colloidal Blue staining Kit (Invitrogen) and all lanes corresponding to 3 sets of time-points were excised in ten bands per lane for enzymatic digestion. A second independent experiment was performed identically except that the cells were serum deprived for 16 h before ligand stimulation.

EGF-dependent interaction partners of PCM1 and WWP2 were identified using a quantitative proteomics strategy described previously.[66] Briefly, for PCM1 two populations of HeLa cells were SILAC labeled with Ly0/Arg0 and Lys4/Arg6, respectively. Five 15 cm dishes from each condition were grown to 90% confluence of the cells and serum starved for 12 h. The Lys4/Arg6-labeled cells were then stimulated with EGF (150 ng ml^{-1}) for 10 min, while the Lys0/Arg0 cells were left untreated. Cells were lysed using the same buffer as above and lysates were incubated with 40 μg of the anti-PCM1 antibody (Abnova Corporation; H00005108-B01) bound to Protein G Sepharose beads to enrich PCM1 with its associated complexes. After 5 h of incubation at 4 °C the beads were mixed, extensively washed with lysis buffer, protein complexes were separated by 1D-gel electrophoresis and further processed for MS analyses as described above. For identification of EGF-dependent interaction partners of WWP2, 30 μg of the WWP2 antibody (Santa Cruz Biotechnology; sc-30052) was used following the same experimental procedure. To evaluate the statistical significance of the PCM1 and WWP2 interacting proteins identified through these quantitative proteomics screens (ESI†, Table S5) we applied a statistical *z*-test as previously described.[67]

Mass spectrometry and data analysis

The excised gel bands were subjected to in-gel reduction, alkylation and trypsin digestion as previously described[68]

and concentrated and desalted using STAGE tips.[69] Concentrated peptide mixtures were analyzed by nano-scale LC–MS/MS as described before[67] using an Agilent 1100 nanoflow system (Agilent Technologies) coupled online to a LTQ-FT Ultra hybrid mass spectrometer (Thermo Fisher Scientific) equipped with a nano-electrospray ion source (Proxeon). The mass spectrometer was operated in the data-dependent mode to automatically switch between MS and MS/MS acquisitions applying the following parameters: full scan mass range m/z 350–1400; resolution $r = 100\,000$; an AGC target of 3 000 000; normalized collision energy, 30%; an activation time of 30 ms and activation $q = 0.25$ for MS2; a dynamic exclusion window of 45 s; an ion selection threshold of 100 counts for MS2. All full scan MS spectra were acquired by the FTICR and the five most intense ions from each scan were sequentially isolated and fragmented in the linear ion trap. Spray voltage was 2.3 kV and capillary temperature was 150 °C.

Raw spectra were merged into a single peak-list file using DTA supercharge v.1.16[70] and searched against the human IPI protein database v.3.32 containing 71 481 sequences with Mascot v.2.2 (Matrix Science). The following search parameters were used: a precursor mass tolerance of 15 ppm and 0.6 Da tolerance for fragments; trypsin enzyme specificity; maximum 2 missed cleavages; fixed modifications: carbamidomethyl (C); variable modifications: oxidation (M), N-term protein acetylation, deamidation (NQ), pyroglutamate (EQ), phosphorylation (STY); and SILAC K4 + K8 + R6 + R10 quantitation mode. The peak-lists were also searched against the corresponding reversed protein database using the same parameters. For identification of proteins we included criteria for at least two unique peptides per protein, peptide mass accuracy below 6 ppm and a mascot score for the proteins not less than 70. MSQuant v.1.4.2[70] were used for quantitation and manual validation where protein ratios are calculated by averaging the ratios of all peptides from the corresponding protein for each stimulation time-point and normalized to the common 0 min time-point as a reference. The GProX software[71] was used for visualization and comparison of profiles.

Confocal microscopy

Serum-starved HeLa cells were fixed in 4% (v/v) formaldehyde for 15 min, permeabilized with 1% (v/v) Triton X-100 for 10 min, and blocked for 30 min with horse serum 1% (v/v) in PBS. Primary and secondary antibody incubations were for 1.5 h and 1 h, respectively, and the cover slips were washed 4 times for 10 min with PBS after each incubation. Cover slips were mounted on glass slides and imaged using a Zeiss LSM 510 Meta Confocal Laser Scanning Microscope. To assess the extent of co-localization of PCM1 and Azi1 in HeLa cells before and after EGF stimulation, immunostaining images were processed using the CellProfiler software (http://www.cellprofiler.org/). A pipeline defying background-to-noise detection threshold was generated and subsequently objects were identified by size, which was applied for all fluorescent images. The co-localization areas were then analyzed by measuring intensities on overlay images and the co-localization ratios before and after EGF stimulation were quantified. All cells in each visualized field (on average 10 cells per field) were used for the measurements. Three images for each condition were used and the statistical significance of the quantified differences was assessed by Paired Student's t-test.

Antibodies used for immunostaining were as follows: rabbit anti-PCM1 (Bethyl Laboratories; A301-149A), mouse anti-PCM1 (Abnova Corporation; H00005108-B01), rabbit anti-Azi1 (Bethyl Laboratories; A301-415A), rabbit anti-MIB1 (Abgent Corporation; AP2172a), rabbit anti-WWP2 (Santa Cruz Biotechnology; sc-30052), mouse anti-EGFR (Transduction Laboratories; E12020), Alexa-488-conjugated anti-rabbit (Molecular Probes), and cyanin-3 (Cy3) conjugated anti-mouse antibodies (Jackson Immuno Labs).

Immunoprecipitation and Western blotting

One 15 cm dish with 90% confluence of the cells per condition was used for the immunoprecipitation (IP) and Western blotting (WB) experiments. Cells were serum-starved for 16 h, left untreated or treated with the EGF for indicated time-periods and lysed as described above. The cleared lysates were incubated with antibodies bound to protein G or A beads for 5 h at 4 °C. The beads were washed 3 times with lysis buffer and immunoprecipitated proteins were resolved on SDS-PAGE and transferred to a nitrocellulose membrane. The membrane was blocked with 2% BSA followed by incubation with primary and HRP-conjugated secondary antibodies (Amersham Pharmacia Biotech) and visualized using the ECL kit as described.[72]

For IP of PCM1 under denaturing conditions, following 16 h serum starvation HeLa cells were stimulated for 10 min with the EGF or left untreated. 1% SDS was added to lysates and incubated on ice for 30 min. Samples were then diluted with lysis buffer to a final concentration of SDS of 0.1% and subjected to immunoprecipitation with an anti-PCM1 antibody as it was described earlier. WB with an anti-Azi1 antibody was used to confirm the loss of PCM1 interaction partners in the IP due to SDS treatment. For the experiments with EGFR tyrosine kinase inhibitor ZD1839 (Iressa), HeLa cells were serum starved for 16 h and treated with ZD1839 (5 μM) or mock treated with DMSO 20 min prior to stimulation with the EGF. IP of Azi1 was performed as described above. ZD1839 was purchased from Selleck Chemicals (S1025). Quantitative measurements of the co-immunoprecipitated PCM1 and AZI1 on the WB images were done using the integrated density function of ImageJ software (http://rsb.info.nih.gov/ij/) in accordance with the program's instructions. Minimum three WB images with different exposure times were measured as indicated (Fig. 3D and E). Paired Student's t-test was applied to assess the statistical significance of the differences of co-immunoprecipitated proteins before and after EGF stimulation.

For the IP and WB experiments described above the following antibodies were used: rabbit anti-EGFR (Santa Cruz; sc-1005), mouse anti-ubiquitin (Santa Cruz; sc-8017), mouse anti-Polyubiquitin Lys-63-linkage-specific (Enzo Life Sciences, HWA4C4), rabbit anti-PCM1 (Bethyl Laboratories; A301-149A), rabbit anti-Azi1 (Bethyl Laboratories; A301-415A), mouse anti-phosphotyrosine, clone 4G10 (Millipore; 05-321).

Acknowledgements

We thank Dr Jakob Bunkenborg, Dr Jacob Schroeder, Maria Nielsen and Lasse Falkenby for technical assistance. We are

grateful to Dr Shao-En Ong and Dr Irina Kratchmarova for critical reading of the manuscript and Prof. Ivan Dikic for GST-UBD constructs. This work was supported by grants from the Danish Natural Sciences Research Council, the European Commission's 7th Framework Program (HEALTH-F4-2008-201648/PROSPECTS) and the Lundbeck Foundation (B.B.—Junior Group Leader Fellowship).

Notes and references

1 C. M. Pickart, *Annu. Rev. Biochem.*, 2001, **70**, 503–533.
2 D. Komander, *Biochem. Soc. Trans.*, 2009, **37**, 937–953.
3 L. Hicke, H. L. Schubert and C. P. Hill, *Nat. Rev. Mol. Cell Biol.*, 2005, **6**, 610–621.
4 K. Haglund and I. Dikic, *EMBO J.*, 2005, **24**, 3353–3359.
5 N. Mailand, S. Bekker-Jensen, H. Faustrup, F. Melander, J. Bartek, C. Lukas and J. Lukas, *Cell*, 2007, **131**, 887–900.
6 T. E. Messick and R. A. Greenberg, *J. Cell Biol.*, 2009, **187**, 319–326.
7 T. K. Pandita and C. Richardson, *Nucleic Acids Res.*, 2009, **37**, 1363–1377.
8 T. Hunter, *Cell*, 2000, **100**, 113–127.
9 T. Pawson, *Cell*, 2004, **116**, 191–203.
10 J. Schlessinger, *Cell*, 2000, **103**, 211–225.
11 Y. L. Deribe, T. Pawson and I. Dikic, *Nat. Struct. Mol. Biol.*, 2010, **17**, 666–672.
12 A. Sorkin and L. K. Goh, *Exp. Cell Res.*, 2009, **315**, 683–696.
13 Y. Zwang and Y. Yarden, *Traffic*, 2009, **10**, 349–363.
14 P. P. Di Fiore, S. Polo and K. Hofmann, *Nat. Rev. Mol. Cell Biol.*, 2003, **4**, 491–497.
15 M. D. Marmor and Y. Yarden, *Oncogene*, 2004, **23**, 2057–2070.
16 D. Hoeller, N. Crosetto, B. Blagoev, C. Raiborg, R. Tikkanen, S. Wagner, K. Kowanetz, R. Breitling, M. Mann, H. Stenmark and I. Dikic, *Nat. Cell Biol.*, 2006, **8**, 163–169.
17 R. Hjerpe and M. S. Rodriguez, *Biochem. Soc. Trans.*, 2008, **36**, 823–827.
18 T. Gururaja, W. Li, W. S. Noble, D. G. Payan and D. C. Anderson, *J. Proteome Res.*, 2003, **2**, 394–404.
19 J. Peng, D. Schwartz, J. E. Elias, C. C. Thoreen, D. Cheng, G. Marsischky, J. Roelofs, D. Finley and S. P. Gygi, *Nat. Biotechnol.*, 2003, **21**, 921–926.
20 J. M. Danielsen, K. B. Sylvestersen, S. Bekker-Jensen, D. Szklarczyk, J. W. Poulsen, H. Horn, L. J. Jensen, N. Mailand and M. L. Nielsen, *Mol. Cell. Proteomics*, 2011, **10**, M110.003590.
21 E. Argenzio, T. Bange, B. Oldrini, F. Bianchi, R. Peesari, S. Mari, P. P. Di Fiore, M. Mann and S. Polo, *Mol. Syst. Biol.*, 2011, **7**, 462.
22 M. Matsumoto, S. Hatakeyama, K. Oyamada, Y. Oda, T. Nishimura and K. I. Nakayama, *Proteomics*, 2005, **5**, 4145–4151.
23 J. Vasilescu, J. C. Smith, M. Ethier and D. Figeys, *J. Proteome Res.*, 2005, **4**, 2192–2200.
24 G. Xu, J. S. Paige and S. R. Jaffrey, *Nat. Biotechnol.*, 2010, **28**, 868–873.
25 R. Meller, S. J. Thompson, T. A. Lusardi, A. N. Ordonez, M. D. Ashley, V. Jessick, W. Wang, D. J. Torrey, D. C. Henshall, P. R. Gafken, J. A. Saugstad, Z. G. Xiong and R. P. Simon, *J. Neurosci.*, 2008, **28**, 50–59.
26 J. W. Pridgeon, T. Geetha and M. W. Wooten, *Biol. Proced. Online*, 2003, **5**, 228–237.
27 S. E. Ong, B. Blagoev, I. Kratchmarova, D. B. Kristensen, H. Steen, A. Pandey and M. Mann, *Mol. Cell. Proteomics*, 2002, **1**, 376–386.
28 J. V. Olsen, B. Blagoev, F. Gnad, B. Macek, C. Kumar, P. Mortensen and M. Mann, *Cell*, 2006, **127**, 635–648.
29 K. T. Rigbolt and B. Blagoev, *Methods Mol. Biol. (Totowa, N. J.)*, 2010, **658**, 187–204.
30 S. Raasi, I. Orlov, K. G. Fleming and C. M. Pickart, *J. Mol. Biol.*, 2004, **341**, 1367–1379.
31 K. Haglund, P. P. Di Fiore and I. Dikic, *Trends Biochem. Sci.*, 2003, **28**, 598–603.
32 F. Huang, D. Kirkpatrick, X. Jiang, S. Gygi and A. Sorkin, *Mol. Cell*, 2006, **21**, 737–748.
33 K. Haglund, S. Sigismund, S. Polo, I. Szymkiewicz, P. P. Di Fiore and I. Dikic, *Nat. Cell Biol.*, 2003, **5**, 461–466.
34 Y. Mosesson, K. Shtiegman, M. Katz, Y. Zwang, G. Vereb, J. Szollosi and Y. Yarden, *J. Biol. Chem.*, 2003, **278**, 21323–21326.
35 T. Woelk, B. Oldrini, E. Maspero, S. Confalonieri, E. Cavallaro, P. P. Di Fiore and S. Polo, *Nat. Cell Biol.*, 2006, **8**, 1246–1254.
36 G. Levkowitz, H. Waterman, E. Zamir, Z. Kam, S. Oved, W. Y. Langdon, L. Beguinot, B. Geiger and Y. Yarden, *Genes Dev.*, 1998, **12**, 3663–3674.
37 W. Chan, R. Tian, Y. F. Lee, S. T. Sit, L. Lim and E. Manser, *J. Biol. Chem.*, 2009, **284**, 8185–8194.
38 A. Magnifico, S. Ettenberg, C. Yang, J. Mariano, S. Tiwari, S. Fang, S. Lipkowitz and A. M. Weissman, *J. Biol. Chem.*, 2003, **278**, 43169–43177.
39 J. S. Andersen, C. J. Wilkinson, T. Mayor, P. Mortensen, E. A. Nigg and M. Mann, *Nature*, 2003, **426**, 570–574.
40 A. Dammermann and A. Merdes, *J. Cell Biol.*, 2002, **159**, 255–266.
41 J. Dengjel, I. Kratchmarova and B. Blagoev, *Methods Mol. Biol. (Totowa, N. J.)*, 2010, **658**, 267–278.
42 C. Choudhary and M. Mann, *Nat. Rev. Mol. Cell Biol.*, 2010, **11**, 427–439.
43 J. Dengjel, I. Kratchmarova and B. Blagoev, *Mol. BioSyst.*, 2009, **5**, 1112–1121.
44 W. Kolch and A. Pitt, *Nat. Rev. Cancer*, 2010, **10**, 618–629.
45 T. Hunter, *Mol. Cell*, 2007, **28**, 730–738.
46 B. Blagoev, S. E. Ong, I. Kratchmarova and M. Mann, *Nat. Biotechnol.*, 2004, **22**, 1139–1145.
47 G. Hudelist, C. F. Singer, M. Manavi, K. Pischinger, E. Kubista and K. Czerwenka, *Breast Cancer Res. Treat.*, 2003, **80**, 353–361.
48 D. E. Hammond, R. Hyde, I. Kratchmarova, R. J. Beynon, B. Blagoev and M. J. Clague, *J. Proteome Res.*, 2010, **9**, 2734–2742.
49 I. Kratchmarova, B. Blagoev, M. Haack-Sorensen, M. Kassem and M. Mann, *Science*, 2005, **308**, 1472–1477.
50 A. E. Lenferink, R. Pinkas-Kramarski, M. L. van de Poll, M. J. van Vugt, L. N. Klapper, E. Tzahar, H. Waterman, M. Sela, E. J. van Zoelen and Y. Yarden, *EMBO J.*, 1998, **17**, 3385–3397.
51 S. K. Muthuswamy, M. Gilman and J. S. Brugge, *Mol. Cell. Biol.*, 1999, **19**, 6845–6857.
52 Z. Wang, L. Zhang, T. K. Yeung and X. Chen, *Mol. Biol. Cell*, 1999, **10**, 1621–1636.
53 M. Itoh, C. H. Kim, G. Palardy, T. Oda, Y. J. Jiang, D. Maust, S. Y. Yeo, K. Lorick, G. J. Wright, L. Ariza-McNaughton, A. M. Weissman, J. Lewis, S. C. Chandrasekharappa and A. B. Chitnis, *Dev. Cell*, 2003, **4**, 67–82.
54 J. Martin-Serrano, S. W. Eastman, W. Chung and P. D. Bieniasz, *J. Cell Biol.*, 2005, **168**, 89–101.
55 F. J. McDonald, A. H. Western, J. D. McNeil, B. C. Thomas, D. R. Olson and P. M. Snyder, *Am. J. Physiol. Renal Physiol.*, 2002, **283**, F431–F436.
56 C. Choudhary, C. Kumar, F. Gnad, M. L. Nielsen, M. Rehman, T. C. Walther, J. V. Olsen and M. Mann, *Science*, 2009, **325**, 834–840.
57 Y. L. Deribe, P. Wild, A. Chandrashaker, J. Curak, M. H. Schmidt, Y. Kalaidzidis, N. Milutinovic, I. Kratchmarova, L. Buerkle, M. J. Fetchko, P. Schmidt, S. Kittanakom, K. R. Brown, I. Jurisica, B. Blagoev, M. Zerial, I. Stagljar and I. Dikic, *Sci. Signaling*, 2009, **2**, ra84.
58 Y. S. Gao, C. C. Hubbert and T. P. Yao, *J. Biol. Chem.*, 2010, **285**, 11219–11226.
59 L. K. Goh, F. Huang, W. Kim, S. Gygi and A. Sorkin, *J. Cell Biol.*, 2010, **189**, 871–883.
60 B. T. Seet, I. Dikic, M. M. Zhou and T. Pawson, *Nat. Rev. Mol. Cell Biol.*, 2006, **7**, 473–483.
61 M. Bartkiewicz, A. Houghton and R. Baron, *J. Biol. Chem.*, 1999, **274**, 30887–30895.
62 J. Liu, S. M. DeYoung, J. B. Hwang, E. E. O'Leary and A. R. Saltiel, *J. Biol. Chem.*, 2003, **278**, 36754–36762.
63 E. Mizuno, K. Kawahata, M. Kato, N. Kitamura and M. Komada, *Mol. Biol. Cell*, 2003, **14**, 3675–3689.
64 B. Blagoev, I. Kratchmarova, S. E. Ong, M. Nielsen, L. J. Foster and M. Mann, *Nat. Biotechnol.*, 2003, **21**, 315–318.
65 B. Blagoev and M. Mann, *Methods*, 2006, **40**, 243–250.
66 K. T. Rigbolt, T. A. Prokhorova, V. Akimov, J. Henningsen, P. T. Johansen, I. Kratchmarova, M. Kassem, M. Mann, J. V. Olsen and B. Blagoev, *Sci. Signaling*, 2011, **4**, rs3.

67 T. A. Prokhorova, K. T. Rigbolt, P. T. Johansen, J. Henningsen, I. Kratchmarova, M. Kassem and B. Blagoev, *Mol. Cell. Proteomics*, 2009, **8**, 959–970.
68 A. Shevchenko, H. Tomas, J. Havlis, J. V. Olsen and M. Mann, *Nat. Protoc.*, 2006, **1**, 2856–2860.
69 J. Rappsilber, Y. Ishihama and M. Mann, *Anal. Chem.*, 2003, **75**, 663–670.
70 P. Mortensen, J. W. Gouw, J. V. Olsen, S. E. Ong, K. T. Rigbolt, J. Bunkenborg, J. Cox, L. J. Foster, A. J. Heck, B. Blagoev, J. S. Andersen and M. Mann, *J. Proteome Res.*, 2010, **9**, 393–403.
71 K. T. Rigbolt, J. T. Vanselow and B. Blagoev, *Mol. Cell. Proteomics*, 2011, **10**, O110.007450.
72 J. Dengjel, V. Akimov, J. V. Olsen, J. Bunkenborg, M. Mann, B. Blagoev and J. S. Andersen, *Nat. Biotechnol.*, 2007, **25**, 566–568.